The laboratory model of the manipulator arm (WMS1 LEMUR) dedicated for on-orbit operation

K. Seweryn, T. Rybus, J. Lisowski, T. Barciński, M. Ciesielska, K. Grassmann, J. Grygorczuk, M. Krzewski, T. Kuciński, J. Nicolau-Kukliński, R. Przybyła, K. Rutkowski, K. Skup, T. Szewczyk, R. Wawrzaszek

Space Research Centre of the Polish Academy of Sciences (CBK PAN), Poland
e-mail: kseweryn@cbk.waw.pl

Abstract

The paper presents the laboratory model of the 7DoF manipulator arm designed to perform automatic on-orbit capture maneuvers during servicing missions. The main objective of the system is to grab the target spacecraft which, in general, can rotate freely in space. Three major subsystems were designed: the mechanics of arm including efficient cycloidal gear, the path planning and control system with input/output lines to spacecraft AOCS, and two dedicated test-bed systems to validate specific aspects of the space manipulator operations.

1 Introduction

Interest in unmanned systems performing the Automatic Rendezvous and Docking or Berthing (RVD/B) task with robotic manipulator has increased recently due to both economic reasons and security concerns. Feasibility studies have shown that large amount of funds can be saved by repairing and servicing the malfunctioned satellites instead of launching new ones ([1] and [2]). Moreover, the increasing number of space debris starts to pose a serious threat to active spacecrafts. *Clean Space* is one of the main current ESA activities addressing this problem. The RVD/B maneuver is a major challenge for space manipulator systems due to high complexity and technological constraints. In contrast to industrial robots, satellite mounted manipulators are free floating – the dynamic interactions between the arm and the spacecraft highly influence system behavior. What is more, stringent mass and power restrictions result in a trade-off between its mass, stiffness of links and joints, and operational workspace.

The main objective of the space manipulator system is to grab the target spacecraft which, in general, can rotate freely (tumbling) in space. Such operation has different phases, e.g., manipulator unfolding, motion toward contact, contact establishing, detumbling and rigidization, and each of the phases have its operation and testing scenario. To fulfill main objective, the following requirements shall be met on the system level: (i) state of the target shall be estimated and predicted accurately by navigation module; (ii) robot's arm trajectory shall be automatically generated with cooperation with AOCS (Attitude and Orbit Control System); (iii) trajectory should be checked against workspace constraints (including dynamic singularities) and executed by control system; (iv) mechanical structure of the robot and drives shall withstand the resulting loads and allow for precise control.

In CBK PAN (Space Research Centre of the Polish Academy of Sciences) a new laboratory model of the manipulator was developed as a result of two-year project "Development and Construction of the Space Manipulator Prototype for On-orbit servicing" funded by the National Center of Research and Development (NCBR) in Poland. The main objective of the project was to build the manipulator arm and to perform preliminary analysis of the system performance with respect to the defined requirements.

Figure 1. Prototype of robotic arm WMS1 LEMUR during integration on the suspension test-bed.

This hardware step was based on CBK previous work, especially availability of Space Robot Simulation Tool [3] and associated algorithms [4] which allows to assist the analysis of robot's dynamics. This software was validated on a developed planar air-bearing test-bed system [5].

The paper presents the laboratory model of the 7DoF manipulator arm designed to perform automatic on-orbit capture maneuvers during servicing or debris removal mission. The next sections cover the description of the control system, manipulator mechanical design and dedicated test-bed systems. The last section covers lesson learned as well as a list of future work.

2 Manipulator control system

Manipulator control system is an integral part of the manipulator arm laboratory model. Control system designed and implemented during the performed project is composed of two main modules: (i) trajectory planning module and (ii) manipulator controller. Trajectory planning module is responsible for planning end-effector trajectory in the inertial reference frame (e.g., trajectory needed for grasping target satellite docking port). It is assumed that the capture maneuver is performed without active attitude and position control, thus free-floating nature of the satellite-manipulator system must be taken into account. From a trajectory defined in the Cartesian space trajectory in the manipulator, the configuration space can be computed using dynamical body Jacobian. The desired trajectory must avoid dynamic singularities of satellite-manipulator system. The second module of the control system is responsible for realization of selected trajectory. For this purpose, Jacobian-based Cartesian control is used (control scheme is based on the fixed-base Jacobian inverse with addition of satellite velocity feedback). PID controllers are responsible for realization of manipulator trajectory in the configuration space.

2.1 Trajectory planning and singularity avoidance

Various methods can be used for trajectory planning of a free-floating manipulator (e.g., [6], [7]). In our approach we solve the path planning problem in the Cartesian space and solve inverse kinematics on the velocity level using the manipulator dynamic Jacobian. For the free-floating manipulator, transformation of a trajectory given in the velocity space to joint velocities requires inverting the body dynamic Jacobian [8]:

$$\dot{\mathbf{q}} = \mathbf{J}_{dyn}^{b\ -1}(\mathbf{q})\mathbf{V}_{ee}^{b}, \tag{1}$$

where $\mathbf{q}$ denotes the vector of configuration coordinates (positions of manipulator joints). In some configurations of the manipulator, Jacobian operator loses rank and we are no longer able to generate any velocity vector in the Cartesian space. Thus, trajectory should be planned in such a way as to avoid singular configurations.

To assess how far the manipulator is from a singular configuration for given positions of joints, we use a manipulability measure defined as:

$$N_{JJ} = \det\left[\mathbf{J}_{dyn}^{b}\left(\mathbf{J}_{dyn}^{b}\right)^{T}\right]. \tag{2}$$

Equation (2) is used to compute a map of the manipulability measure in the configuration space. Such map, for a 7 DoF WMS-1 LEMUR manipulator, is shown in the Fig. 2, on which only configurations with low manipulability are presented (manipulability equals zero for singular configurations). Maps of manipulability measure for various possible configurations of manipulator were presented in [9].

For a trajectory of the end-effector velocity given in Cartesian coordinates of the inertial reference frame, we have to numerically integrate (1) in order to obtain trajectory in the configuration space and to assess whether this trajectory would drive the system to one of its dynamically singular configurations. The trajectory from the initial to the final position of the end-effector can be defined by parametric curve. The alteration of curve shape will result in altered end-effector trajectory in the velocity space and different path in the joint space. Changing curve shape would, therefore, allow avoidance of dynamic singularities of the satellite-manipulator system. In our approach, we use Bézier curve to define trajectory between initial and final end-effector position [10]. In three dimensional space third-order Bézier curve has the following form:

$$\mathbf{P}(n) = (1-n)^3\mathbf{P}_b + 3(1-n)^2 n\mathbf{P}_1 + 3(1-n)n^2\mathbf{P}_2 + n^3\mathbf{P}_e, \tag{3}$$

where $n \in [0;1]$ and curve is characterized by four points: initial position $\mathbf{P}_b$, final position $\mathbf{P}_e$ and two intermediate points ($\mathbf{P}_1$ and $\mathbf{P}_2$). The curve starts at $\mathbf{P}_b$ going towards $\mathbf{P}_1$ and arrives at $\mathbf{P}_e$ coming from the direction of $\mathbf{P}_2$ (intermediate points do not lie on the curve, but they determine its shape). Positions of the intermediate points can be described with respect to the end-effector initial and final position by parameters such as angles and distances to the points. The selection of these parameters (responsible for curve shape) is

intuitive and can be performed by automatic algorithm. In the Fig. 3, Bézier curve trajectory is compared with straight line trajectory for 7 DoF free-floating manipulator. Positions of manipulator joints are shown in the Fig. 4, where at some point configuration close to singular is reached for straight line trajectory and body dynamic Jacobian in (1) cannot be inverted. Driving torque applied in manipulator joints during realization of Bézier curve trajectory are shown in the Fig. 5, while frames from animation presenting satellite-manipulator system during realization of this trajectory are shown in the Fig. 6.

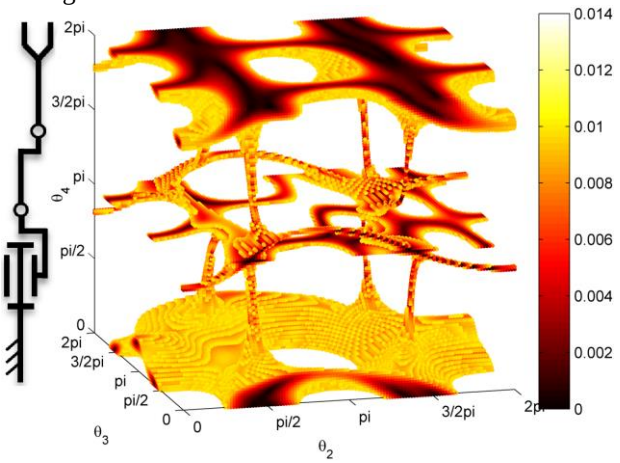

Figure 2. Kinematic scheme of the 7 DoF WMS-1 LEMUR manipulator (only four joints are presented) and manipulability measure for this manipulator.

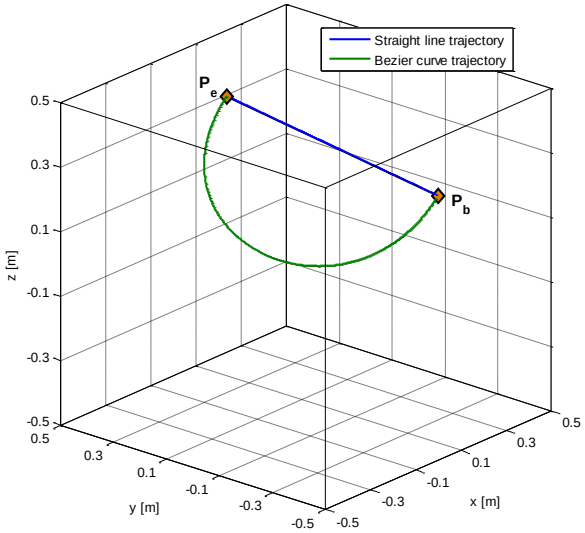

Figure 3. Straight line and Bézier curve trajectory.

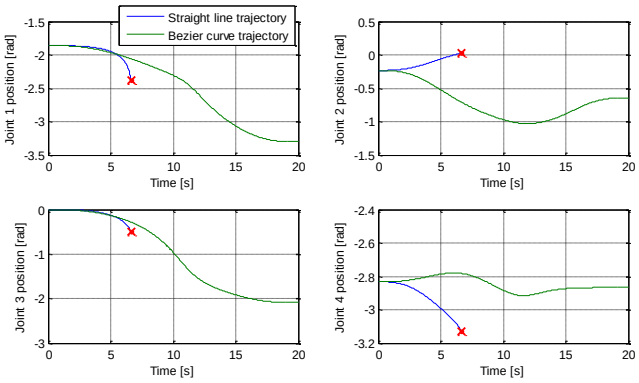

Figure 4. Positions of first four manipulator joints for straight line and Bézier curve trajectory (results of numerical simulations).

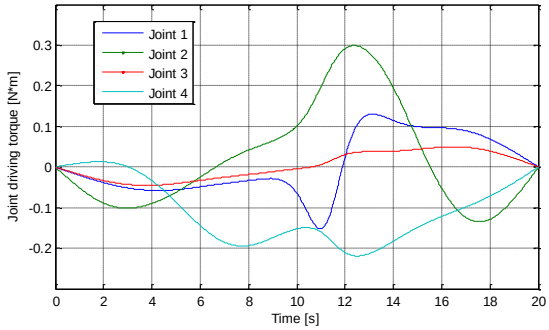

Figure 5. Driving torque applied in manipulator joints for Bézier curve trajectory.

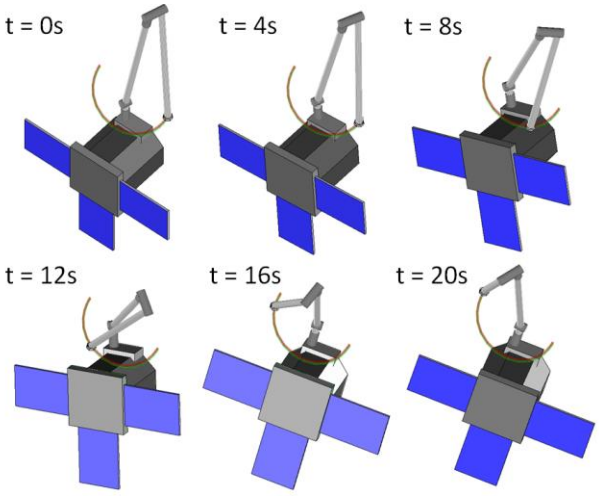

Figure 6. Frames from animation presenting satellite-manipulator system during realization of Bézier curve trajectory.

2.2 Manipulator controller

The control of the manipulator mounted on the free-floating satellite is a challenging task as dynamic interactions between the manipulator and the satellite must be taken into account. Use of the control law based on (1) is difficult due to the high computational cost of the dynamic body Jacobian calculation. Thus, we proposed to use simple and computationally cheap kinematic control (based on geometric body Jacobian that does not take into account free-floating nature of the satellite manipulator system) with addition of satellite velocity feedback, i.e., feedback from measurements of manipulator-base velocity:

$$\dot{\mathbf{q}}_{ref} = \mathbf{J}_{dyn}^{b\ -1}(\mathbf{q})(\mathbf{V}_{ee\,ref}^{b} - Ad_{g^{-1}}\mathbf{V}_{SC}), \qquad (4)$$

where $\mathbf{V}_{ee\,ref}^{b}$ is the end-effector velocity on reference trajectory (in inertial reference frame), $\mathbf{V}_{SC}$ is the satellite body velocity, Ad_f is adjoint operator of f and g is the end effector configuration with respect to the satellite. The presented control scheme was compared with other Cartesian control algorithms and it was demonstrated that for nominal parameters its performance is similar to the performance of the inverse dynamical Jacobian control, while computational effort is lower [11]. In the Fig. 7 position of the end-effector obtained from numerical simulations is shown.

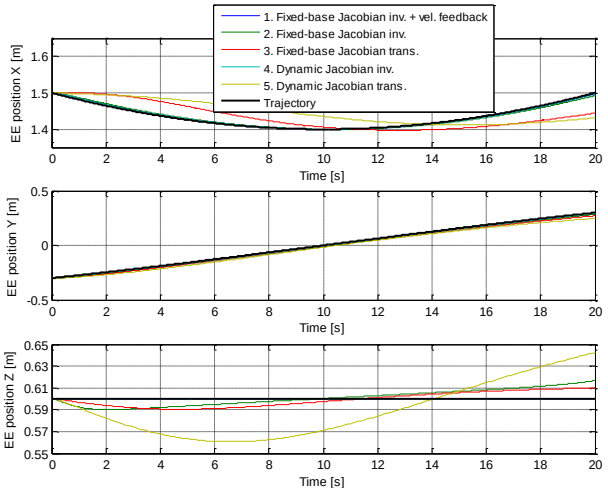

Figure 7. End-effector position during realization of a typical trajectory (results of numerical simulations).

2.3 Implementation of the control system

In the laboratory model of the manipulator arm, control system was implemented on two kinds of electronic circuits: (i) On Board Computer (OBC) and (ii) joint-controller boards (JC). The OBC performs trajectory planning and mode management. It also monitors, collects and stores all the data that comes from the executive subsystems (data logging up to 100 samples/s). Control signals calculated by OBC are sent to joint-controller boards. OBC bases on a 1GHz DM3730 Texas Instruments processor. Application software and all collected data are stored on Flash and SD cards. The joint-controller circuit consists of 32bits ARM Cortex M3 microcontroller, linear power converter, set of input/output buffers and interface to communicate with the encoders. JC boards are responsible for: control of manipulator drives, monitoring positions of manipulator joints and monitoring own electronics by collecting the data about the temperatures, supply current and voltage. Logical blocks of JC are presented in the Fig. 8.

CAN bus at 1Mbps is used for communication between OBC and joint-controllers. Special purpose CAN application level interface has been implemented on top of CAN bus to provide real time and robust transmission channel between systems nodes. It is responsible for transferring reference signals from trajectory planning module of the control system to specific joint control software and for transferring measured joint position from joint-controllers to OBC.

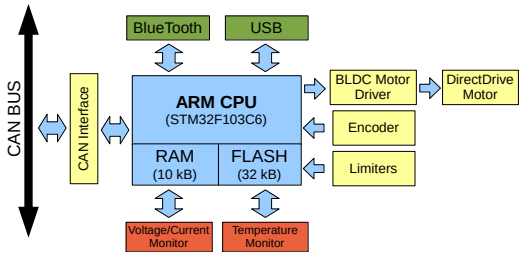

Figure 8. The logical blocks of joint-controller.

3 Manipulator design

A serial manipulator arm type was chosen for analysis. This type of the manipulator consists of links, joints and interfaces between them. The configuration was analyzed at the first stage of the project by analyzing its dynamical behavior during typical on-orbit tasks. The final solution is classical 7DoF elbow-like architecture with total length of 3.1m (Fig. 9). The P1, P2, and P4 is responsible for end effector positioning while the P5, P6 and P7 allows setting specific orientation of the end effector. The P4 joint adds redundancy to the system as well as helps in omitting the singularities in manipulator workspace. The specific for that type of manipulator is the load which is more or less equal over the length of the manipulator. It is a consequence of the lack of gravity and comparable masses attached to both ends of the

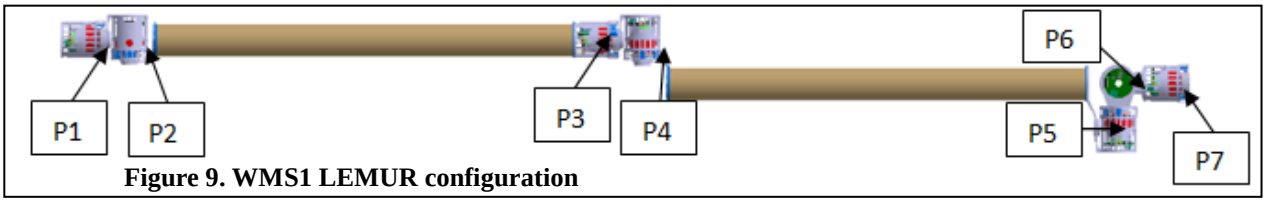

Figure 9. WMS1 LEMUR configuration

manipulator. As a result the size of the links and all joints are similar respectively. It is also important to indicate that manipulator subsystem (joints and links) was designed to operate in on-orbit environment which means that it is not strong enough operate in normal gravity. On the other hand such approach allows minimizing the mass of the system and maximizing the workspace.

3.1 Links

Manipulator links (Fig. 10) are made of carbon fiber composite material. The chosen solution is based on one high modulus tape (90) and two carbon sleeves (45-45) and resulted in the maximum deflection of ~6mm under nominal load in reference scenario and high torsional stiffness. A single link mass is 1kg, whereas the whole mass of the manipulator is less than 20kg. The workspace of the manipulator is half sphere with diameter of about 6.2m.

Figure 10. Manipulator links made of high modulus carbon fiber reinforced materials with interfaces and attachment for tests-bed systems

3.2 Joint with epicycloidal gearhead

The design of the joint (Fig. 11) is based on the torque motor, backlash-free epicycloid gear [13] and control electronics. The selection of the gear was justified by the fact that the transmission occurs only through rolling friction which is preferable solution from tribological point of view especially in space environment. The torque motor was chosen as it has the ability to generate high torque at very low speed, which is highly desirable in robotic applications. Both the chosen gear and the motor allow having a central placed hole with a large diameter and makes routing the cables inside the joint possible. In order to control position, speed and torque the joint has been equipped with sensors and dedicated control unit.

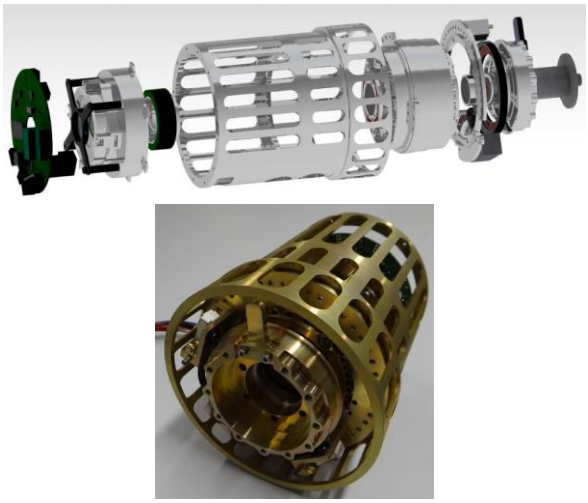

Figure 11. Element of the joint (top view) and the breadboard (bottom view).

The cycloidal gear was chosen as a solution for space robot's joint due to the fact that it fulfills the requirements of minimum mass, maximum efficiency and possibility to operate in space environment. The gear consists of four main components (Fig. 12): an input and output shaft, cycloid disc and housing with internal pins. The input shafts has eccentric surface on which the cycloid disc is mounted. This eccentricity causes the center of the disc to rotate in the housing. There are less wheels teeth than housing's pins, causing the reverse orbit rotation within the housing. The rotary motion is converted via the disc rolling over within the housing, which accommodates the rollers. The reduced rotation is transmitted to the output shaft LSS via pins that engage with holes contained within the cycloid disc. All of the mentioned interactions are based only on rolling one element wrt. others which eliminates the sliding friction problem as well as elasticity of the structural element of the gear which can have an important impact on tribological aspects.

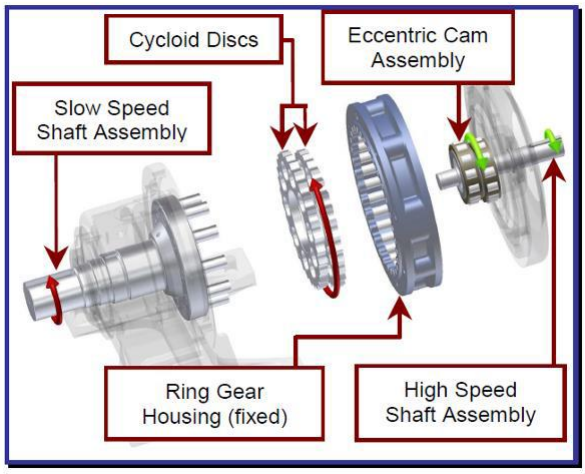

Figure 12. Graphical representation of the cycloid gear principle of operation [13]

The mass of the reducer equals 500g, but the 20% of this mass is the weight of the cross roller bearing on the output shaft. The total weight of the joint equals 1500 g. The developed joint and the cycloid gear is presented in the Fig. 13. The surface on cycloid disc was exposed to hard anodizing to increase the durability. This treatment of the surface, in the future will allow us to moisten it, e.g. with molybdenum disulphide, to improve the tribology parameters in vacuum conditions.

Figure 13. Cycloid gear laboratory model.

3.3 End-effector

The manipulator end effector (Fig. 14) is composed of three joints with axes perpendicular to each other. It is typical solution which helps to decouple the end effector positioning and orientating task. The less typical is the size of the joints (P5, P6 and P7) which are the same as joint responsible for manipulator positioning. Such solution was chosen due to the fact that typically in space operations either of manipulator end can be connected to the higher mass and in consequence the highest torque can appear on both manipulator ends. For example during the debris grasping and deorbiting, the first manipulator is connected only to the chaser satellite however after grasping the both ends are connected to comparable mass.

Figure 14. The laboratory model of the end-effector.

4 Tests-bed systems

Testing the space manipulators is a difficult task in laboratory conditions due to lack of ability to totally eliminate gravity influence on the system behavior. The best solution would be to have laboratory on-orbit; however, the cost of its maintenance would be extremely high. Therefore, the testing systems are often highly integrated with the testing object to validate only specific response of the system which later can be used to estimate parameters obtainable in on-orbit test-bed system.

The WMS1 LEMUR manipulator was also equipped with two dedicated test-bed systems. Planar air bearing test-bed system was dedicated to 2D zero gravity tests of two link manipulator attached to the spacecraft mock-up. This test-bed allowed us to check the manipulator arm control system, especially the feed forward term based on path planning algorithm and spacecraft velocity feedback. The second, suspension test-bed system was dedicated to check the mechanical subsystem of the manipulator as well control system but in this case only the microprocessor ability to execute the floating point operations (Jacobian inverse) in real time was checked.

4.1 Planar air-bearing test-bed

The microgravity simulator designed and developed in the Space Research Centre PAS consists of three elements: (i) air bearing table (ii) 2DoF manipulator mounted on a base (satellite mock-up) and (iii) vision system (Fig. 15). The details were provided by Rybus et al. (2013) on ASTRA conference. System can move and rotate freely on a plane, thus motions of the manipulator will affect position and orientation of the base. Area of the granite table, on which satellite-manipulator system can move, has dimensions of 2x3 meters and is larger than in many similar solutions. The large size of this area allows tests of complex maneuvers and gives possibility of future application of flexible manipulator links. Additional air-bearings are used to support independently each manipulator link, thus allowing tests of long and heavy manipulator (longer and heavier manipulator has more significant influence on base position and orientation). The picture of aforedescribed test-bed is shown in the Fig. 15. The total length of the manipulator is 1.22 m, while mass of the entire system is 18.9 kg.

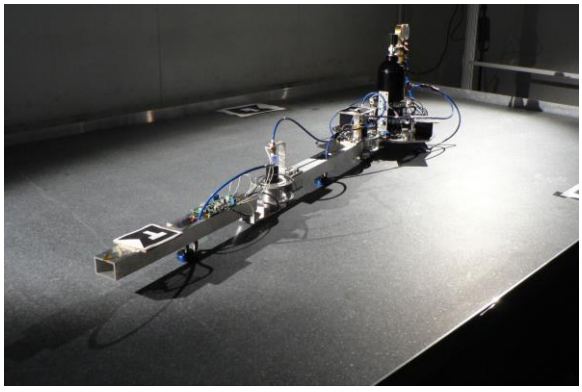

Figure 15. Planar air-bearing microgravity simulator.

The first results of the test realized using this manipulator show that the control system are able to perform any path in Cartesian space and the results were well correlated with the simulation [10].

4.2 Suspension test-bed

Suspension system allows to reduce the first order effect of the gravity influence on the manipulator. This includes the 90% reduction of the gravity force imposed on the not connected link with the appropriate joint. The system contains two follow up extension arms (Fig. 16): the first one (4) dedicated to reduce the gravity influence on first link, the second (3) – for second link and end-effector. Each extension arm has one rotary (10) and one linear joint (11). The axis of rotation on both joints are in line with the first axis of rotation of the first joint. The linear joint allows the special cart (7) where the cord is mounted to move. Through this cord, the force to the link via special interface (see Fig. 16 right bottom) is applied. The linear and rotary joints, as well as the force applied to cord, is actively controlled (12). The camera mounted on cart (7) and measurement spring (6) are used as a sensor to determinate the rotary, linear joint motion as well as to apply constant force (5) to the cord during manipulator arm motion. The system imposes some constraints on manipulator motion mainly connected with its speed which cannot be higher than 2.5m/s horizontally and 1.3 m/s vertically.

Currently the manipulator is tested and the results are planned to be published in close future.

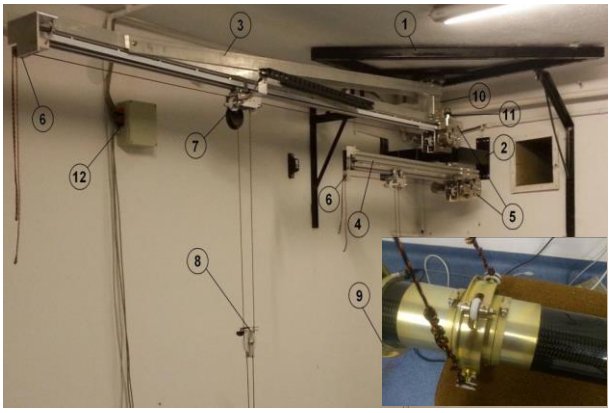

Figure 16. The suspension test-bed for reduction of gravity influence on the manipulator.

5 Conclusions

In the paper the WMS1 LEMUR manipulator arm design and laboratory model is presented. The system design was chosen in such way to be optimal for operation in on-orbit environment, especially for servicing operations and debris removal. The control system has three major features: path planning algorithm providing the feed forward term for controller, the singularity avoidance algorithm which takes advantage of additional joint, smoothly moves through the singularities points and made the system most robust, and control scheme which takes into account cooperation with spacecraft AOCS. The mechanical design of the manipulator was also fitted to the defined requirements, mainly:

- workspace maximization through relatively high length of the manipulator links,
- mass minimization through special design of the

joints equipped with cycloidal gear,
- joint size dedicated for on-orbit operations where on both side of the manipulator the comparable mass can be attached,
- joint design with central hole which helps in cabling.

In addition, two dedicated test-bed systems were designed to test the manipulator arm.

In the future two major investigations are planned: first connected with replacement of the mechanical meshing between gear elements for magnetic ones. This approach is mainly driven by the fact that it will reduce the manufacturing accuracy requirements but increase the flexibility; however, at the same time there are new control algorithms applicable for elastic joints which are able to resolve this issue. The second activity is connected with usage of tubular booms as a structure of links [14]. This brings the possibility to have a manipulator with reconfigurable length which helps mainly with accommodation of the manipulator on spacecraft.

Acknowledgements

The new developed manipulator is a result of 2-year LIDER project "Development and Construction of the Space Manipulator Prototype for On-orbit servicing" project no. LIDER/10/89/L-2/10/NCBIR/2011 which was founded by National Center of Research and Development (NCBR) in Poland.

References

[1] C. Cougnet, et al., "On-orbit servicing system of a GEO satellite fleet", in Proc. of the ASTRA 2006, ESTEC, Noordwijk, The Netherlands, 2006.

[2] J. Kreisel, "On-Orbit servicing of satellites (OOS): its potential market & impact", in Proc. of the ASTRA 2002, ESTEC, Noordwijk, The Netherlands, 2002.

[3] T. Rybus and K. Seweryn, "Trajectory Planning and Simulations of the Manipulator Mounted on a Free-Floating Satellite", in: J.Z. Sasiadek (ed) Aerospace Robotics, GeoPlanet: Earth and Planetary Sciences. Springer-Verlag, 2013.

[4] K. Seweryn and M. Banaszkiewicz, "Optimization of the trajectory of an general free – flying manipulator during the rendezvous maneuver", in Proc. of the AIAA Guidance, Navigation and Control Conference and Exhibit, Honolulu, Hawaii, USA, 2008.

[5] T. Rybus, et al., "New Planar Air-bearing Microgravity Simulator for Verification of Space Robotics Numerical Simulations and Control Algorithms", in Proc. of the ASTRA 2013, ESTEC, Noordwijk, The Netherlands, 2013.

[6] Y. Nakamura and R. Mukherjee, "Nonholonomic Path Planning of Space Robots via Bi-Directional Approach", Transaction on Robotics and Automation, Vol. 7, No. 4, 1991.

[7] C. Li, B. Liang, and W. Xu, "Autonomous Trajectory Planning of Free-floating Robot for Capturing Space Target", in Proc. of the 2006 IEEE/RSJ International Conference on Intelligent Robots and Systems, Beijing, China, 2006.

[8] E. G. Papadopoulos, "Nonholonomic behavior in free-floating manipulators and its utilization", in Nonholonomic motion planning, Kluwer Academic Publishers, 1993.

[9] T. Rybus, et al., "Numerical simulations and analytical analyses of the orbital capture manoeuvre as a part of the manipulator-equipped servicing satellite design", in Proc. of the MMAR 2012, Miedzyzdroje, Poland, Aug. 2012.

[10] T. Rybus, et al., "Experimental demonstration of singularity avoidance with trajectories based on the Bézier curves for free-floating manipulator", in Proc. of the RoMoCo 2013, Wasowo, Poland, 2013.

[11] T. Rybus, et al., "Analyses of a free-floating manipulator control scheme based on the fixed-base Jacobian with spacecraft velocity feedback", in: J. Z. Sasiadek (ed) Aerospace Robotics II, GeoPlanet: Earth and Planetary Sciences. Springer-Verlag, 2014 (in print).

[12] T. Rybus, et al., "Dynamic simulations of free-floating space robots", in: K.R. Kozłowski (ed) Robot Motion and Control 2011, Lecture Notes in Control and Information Sciences. Vol. 422, Springer-Verlag, 2012.

[13] K. Seweryn, et al., "Optimization of the Robotic Joint Equipped with Epicyloidal Gear and Direct Drive for Space Applications," in Proc. of the ESMATS 2013, ESTEC, Noordwijk, The Netherlands, 2013.

[14] T. Kuciński, et al., "Deployable manipulator technology with application for UAVs", in: J. Z. Sasiadek (ed) Aerospace Robotics II, GeoPlanet: Earth and Planetary Sciences. Springer-Verlag, 2014